CHEMISTRY
A EUROPEAN JOURNAL

DOI: 10.1002/chem.200701420

Accelerating and Decelerating Effects of Metal Ions on Electron-Transfer Reduction of Quinones as a Function of Temperature and Binding Modes of Metal Ions to Semiquinone Radical Anions

Junpei Yuasa, Shunsuke Yamada, and Shunichi Fukuzumi*[a]

Abstract: The accelerating effect of Sc^{3+} on the electron-transfer (ET) reduction of the *p*-benzoquinone derivative 1-(*p*-tolylsulfinyl)-2,5-benzoquinone (TolSQ) by 10,10′-dimethyl-9,9′-biacridine ($(AcrH)_2$) at 233 K changes to a decelerating effect with increasing reaction temperature; the observed second-order rate constant k_{et} decreases with increasing Sc^{3+} concentration at high concentrations of Sc^{3+} at 298 K. At 263 K the k_{et} value remains constant with increasing Sc^{3+} concentration. Such a remarkable difference with regard to dependence of k_{et} on $[Sc^{3+}]$ between low and high temperatures results from the difference in relative activity of two ET pathways that depend on temperature, one of which affords 1:1 complex $TolSQ^{\bullet-}$–Sc^{3+}, and the other 1:2 complex $TolSQ^{\bullet-}$–$(Sc^{3+})_2$ with additional binding of Sc^{3+} to $TolSQ^{\bullet-}$–Sc^{3+}. The formation of $TolSQ^{\bullet-}$–Sc^{3+} and $TolSQ^{\bullet-}$–$(Sc^{3+})_2$ complexes was confirmed by EPR spectroscopy in the ET reduction of TolSQ in the presence of low and high concentrations of Sc^{3+}, respectively. The effects of metal ions on other ET reactions of quinones to afford 1:1 and 1:2 complexes between semiquinone radical anions and metal ions are also reported. The ET pathway affording the 1:2 complexes has smaller activation enthalpies $\Delta H^{\neq}$ and more negative activation entropies $\Delta S^{\neq}$ because of stronger binding of metal ions and more restricted geometries of the ET transition states as compared with the ET pathway to afford the 1:1 complexes.

Keywords: electron transfer · kinetics · quinones · radical ions · reduction

Introduction

Activation and deactivation of electron transfer (ET) plays a vital role in controlling biological redox reactions such as photosynthesis and respiration, which are essential for life.[1,2] Electron-transfer reactions are often regulated and tuned through noncovalent interactions (e.g., hydrogen bonds,[3–5] interactions in proteins,[6] electrostatic interactions with metal ions[7–15]) in many biological and chemical redox systems. In particular, metal ions acting as Lewis acids are known to activate ET reactions when they bind to the product radical anions.[7–15] Electron-transfer rates are generally determined by the enthalpies $\Delta H^{\neq}$ and entropies $\Delta S^{\neq}$ of activation. In adiabatic ET reactions in solution, the $\Delta S^{\neq}$ value is normally close to zero, and ET is enthalpy-controlled.[16,17] When ET from an electron donor (D) to an electron acceptor (A) is activated by binding of metal ions (M^{n+}) with the product radical anion ($A^{\bullet-}$), the $\Delta S^{\neq}$ value takes on a large negative value because of restricted geometry in binding of metal ions in the transition state, whereas the $\Delta H^{\neq}$ value becomes smaller because metal-ion binding thermodynamically stabilizes the product radical anion (Scheme 1). If the binding mode of the metal ion complex changes from a 1:1 complex ($A^{\bullet-}$–M^{n+}) to a 1:2 complex ($A^{\bullet-}$–$(M^{n+})_2$) with increasing metal-ion concentration, the $\Delta H^{\neq}$ and $\Delta S^{\neq}$ values would be different for the two binding modes (Scheme 1).[7–15,18,19] In such a case, the rate of the ET pathway to afford 1:2 complex $A^{\bullet-}$–$(M^{n+})_2$ with a smaller $\Delta H^{\neq}$ value and a more negative $\Delta S^{\neq}$ value would be faster than that to afford a 1:1 complex $A^{\bullet-}$–M^{n+} at lower temperature, whereas this would be reversed at higher temperature. This indicates that the ET rate increases with increasing concentration of metal ions at lower temperature, but the ET rate decreases with increasing concentration of metal ions at higher temperature. However, such acceleration and decel-

[a] Dr. J. Yuasa, S. Yamada, S. Fukuzumi
Department of Material and Life Science
Graduate School of Engineering
Osaka University and SORST (JST)
2-1 Yamada-oka, Suita, Osaka 565-0871 (Japan)
Fax: (+81) 6-6879-7370
E-mail: fukuzumi@chem.eng.osaka-u.ac.jp

Supporting information for this article is available on the WWW under http://www.chemistry.org or from the author.

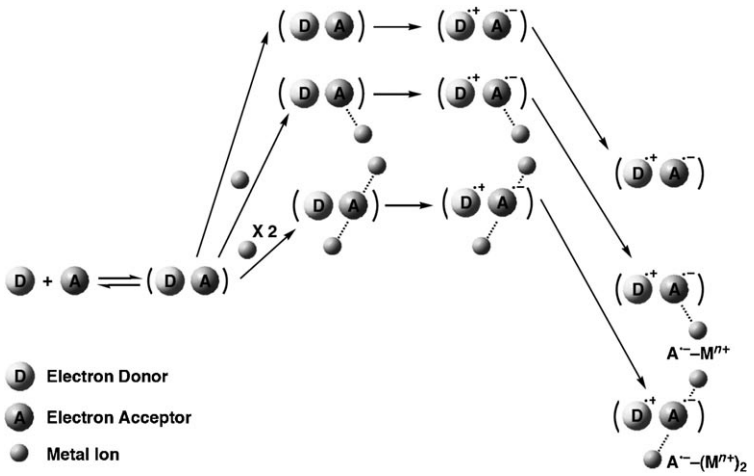

Scheme 1. Schematic description of metal-ion-promoted ET.

eration effects of metal ions on electron transfer depending on temperature have yet to be scrutinized.

We report herein for the first time the accelerating and decelerating effects of metal ions on the ET reduction of *p*- and *o*-quinones, 1-(*p*-tolylsulfinyl)-2,5-benzoquinone (TolSQ) and 9,10-phenanthrenequinone (PQ), by electron donors with different electron-donor abilities ($(AcrH)_2$, [Ir(ppy)$_3$], CoTPP) as a function of temperature. Quinones are known to play a crucial role in biological redox systems.[20–22] TolSQ and PQ were chosen as electron acceptors, because these quinones have metal-ion binding sites for complexation of metal ions. Typically, Sc^{3+} and Y^{3+}, which act as strong Lewis acids, can form complexes with TolSQ and PQ, respectively.[23] Hence, we employed Sc^{3+} and Y^{3+} to demonstrate the accelerating and decelerating effects of metal ions on ET reduction of quinones.

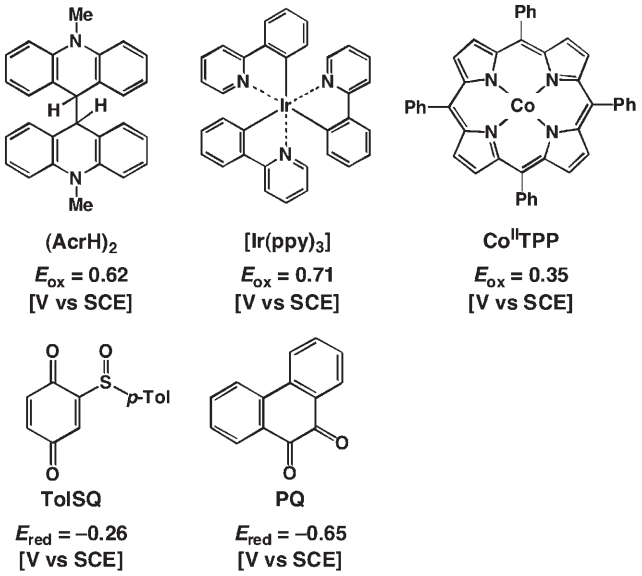

Results and Discussion

Accelerating and decelerating effects of Sc^{3+} on ET from $(AcrH)_2$ to TolSQ: No electron transfer (ET) from 10,10′-dimethyl-9,9′-biacridine ($(AcrH)_2$, $E_{ox}=0.62$ V versus SCE)[24] to 1-(*p*-tolylsulfinyl)-2,5-benzoquinone (TolSQ, $E_{red}=-0.26$ V versus SCE)[25] occurs in acetonitrile (MeCN) at 298 K, in agreement with the highly positive free-energy change of ET ($\Delta G_{et}=0.88$ eV). In the presence of 1.0 M scandium triflate [Sc(OTf)$_3$] (OTf = OSO_2CF_3), however, the reduction potential of TolSQ is shifted to 0.70 V (versus SCE),[25] and efficient ET from $(AcrH)_2$ to TolSQ then occurs to yield 2 equiv of $AcrH^+$ [Eq. (1)]. Hereby, initial ET from $(AcrH)_2$ to TolSQ is followed by facile C–C bond cleavage to give $AcrH^+$ and $AcrH^{\bullet}$ ($E_{red}=-0.46$ V versus SCE),[26] which is a much stronger electron donor than $(AcrH)_2$.[24] Thus, subsequent ET from $AcrH^{\bullet}$ to TolSQ occurs rapidly to yield two equivalents of $AcrH^+$ [Eq. (1)].

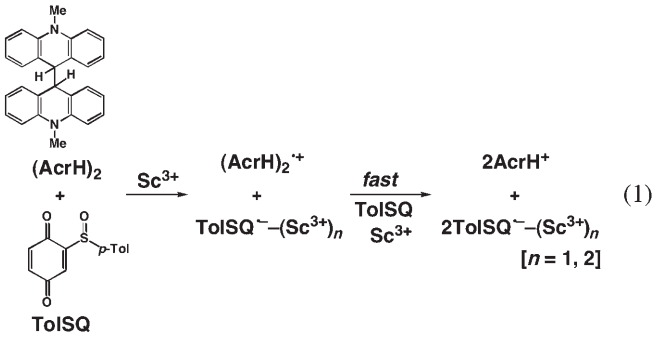

(1)

The ET rate was determined by monitoring the increase in the absorption band due to $AcrH^+$ in deaerated MeCN. The rates obeyed pseudo-first-order kinetics in the presence of a large excess of TolSQ and Sc^{3+} relative to the concentration of $(AcrH)_2$ (see the first-order plots in Figure S1 in the Supporting Information). The dependence of the observed second-order rate constant k_{et} on [Sc^{3+}] for ET from $(AcrH)_2$ to TolSQ at 233 and 298 K is shown in Figure 1a and b, respectively. The k_{et} value increases with increasing Sc^{3+} concentration and exhibits saturation behavior at low concentrations of Sc^{3+} ([Sc^{3+}] $<5.0\times10^{-3}$ M) at both 233 and 298 K (Figure 1a and b, respectively). The saturation dependence of k_{et} on [Sc^{3+}] is ascribed to 1:1 complex formation between TolSQ and Sc^{3+} (TolSQ–Sc^{3+}), which enhances the electron-acceptor ability of TolSQ.[25] The formation constants K_1 of the TolSQ–Sc^{3+} complex at 298 and 233 K

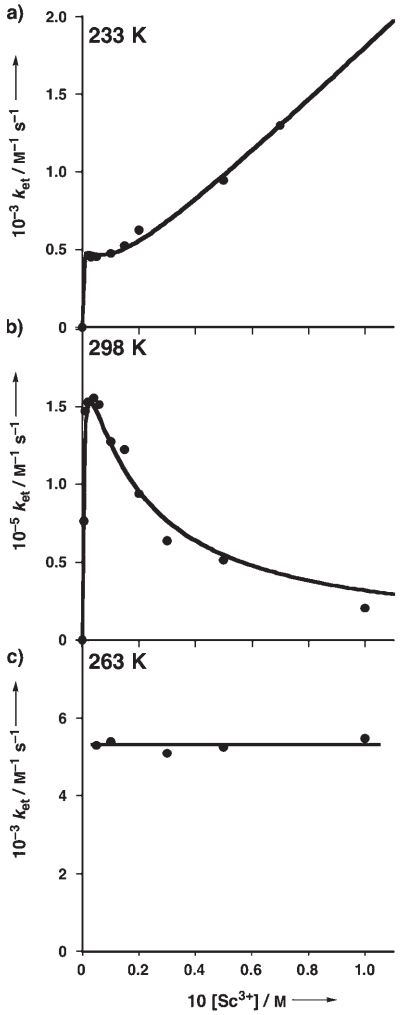

Figure 1. Dependence of k_{et} on [Sc^{3+}] for ET from $(AcrH)_2$ (1.0×10^{-5} M) to TolSQ in the presence of Sc^{3+} in deaerated MeCN at a) 233 K, b) 298 K, and c) 263 K.

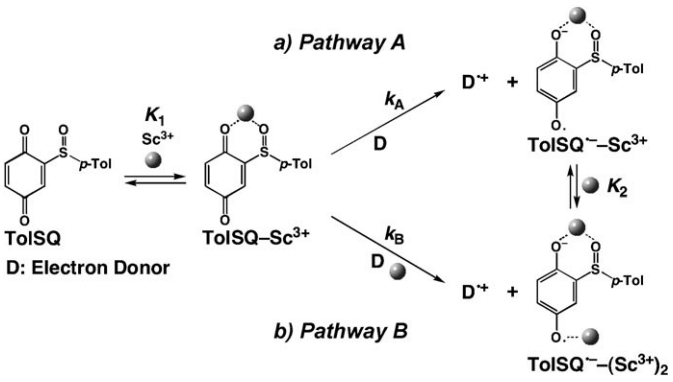

Scheme 2. ET from electron donors to TolSQ–Sc^{3+} to produce a) $TolSQ^{\bullet-}$–Sc^{3+} and b) $TolSQ^{\bullet-}$–$(Sc^{3+})_2$.

were determined from UV/Vis spectral changes of TolSQ in the presence of various concentrations of Sc^{3+} in MeCN as $(2.5\pm0.1)\times10^3\ M^{-1}$ and $(9.7\pm0.1)\times10^3\ M^{-1}$ at 298 and 233 K, respectively.[25]

The k_{et} value increases further with increasing [Sc^{3+}] at high concentrations of Sc^{3+} ([Sc^{3+}] $>5.0\times10^{-3}$ M) at 233 K as shown in Figure 1a. In sharp contrast, the k_{et} value decreases with increasing [Sc^{3+}] at high concentrations of Sc^{3+} ([Sc^{3+}] $>5.0\times10^{-3}$ M) at 298 K (Figure 1b). On the other hand, the k_{et} value is rather constant irrespective of Sc^{3+} concentration at 263 K (Figure 1c). The decelerating effect of metal ions M^{n+} on the rate of ET normally results from complex formation between electron donor and metal ion ($D–M^{n+}$), which reduces the electron-donor ability and decelerates the ET reaction.[27] However, it was confirmed that Sc^{3+} has no effect on the oxidation potential of $(AcrH)_2$.

The accelerating effect of Sc^{3+} on k_{et} in Figure 1a can be easily explained by two ET pathways to produce the 1:1 complex $TolSQ^{\bullet-}$–Sc^{3+} and the 1:2 complex $TolSQ^{\bullet-}$–$(Sc^{3+})_2$ (pathways A and B, respectively, in Scheme 2). No ET from $(AcrH)_2$ to TolSQ occurs without Sc^{3+} (vide supra). In the presence of Sc^{3+}, ET becomes possible by 1:1 complex formation between TolSQ and Sc^{3+} (TolSQ–Sc^{3+}) to afford the $TolSQ^{\bullet-}$–Sc^{3+} complex. With increasing concentration of Sc^{3+}, the 1:1 complex $TolSQ^{\bullet-}$–Sc^{3+} is further converted to the 1:2 complex $TolSQ^{\bullet-}$–$(Sc^{3+})_2$ (pathway B). In such a case, the ET rate increases with increasing concentration of Sc^{3+}, because additional Sc^{3+} is involved in the transition state of ET to afford the 1:2 complex $TolSQ^{\bullet-}$–$(Sc^{3+})_2$.

The dependence of the formation of the 1:1 complex $TolSQ^{\bullet-}$–Sc^{3+} and the 1:2 complex $TolSQ^{\bullet-}$–$(Sc^{3+})_2$ on Sc^{3+} concentration was monitored by EPR spectroscopy in ET from $(AcrH)_2$ to TolSQ in the presence of low and high concentrations of Sc^{3+} (vide infra).[25,28] The EPR spectrum of a deaerated MeCN solution of $(AcrH)_2$ and TolSQ in the presence of a low concentration of Sc^{3+} (4.2×10^{-3} M), shown in Figure 2a, is well reproduced by the simulated spectrum with the hfc values of $a(2H)=1.85$, 0.62 G and superhyperfine splitting due to one Sc^{3+} ion ($a(Sc^{3+})=1.63$ G; Figure 2b).[25,29] This indicates that $TolSQ^{\bullet-}$ forms a 1:1 complex with Sc^{3+} ($TolSQ^{\bullet-}$–Sc^{3+}) in the presence of a low concentration of Sc^{3+}. In the presence of a high concentration of $Sc(OTf)_3$ (2.1×10^{-1} M), the hyperfine pattern changes and exhibits splitting due to the additional Sc^{3+} ion (Figure 2c).[25,28] This indicates that the $TolSQ^{\bullet-}$–Sc^{3+} complex is converted to the 1:2 complex with Sc^{3+} ($TolSQ^{\bullet-}$–$(Sc^{3+})_2$) in the presence of high concentrations of Sc^{3+}.

The activation parameters are expected to differ between pathway A and pathway B, because pathway B to afford $TolSQ^{\bullet-}$–$(Sc^{3+})_2$ may have a smaller activation enthalpy $\Delta H^{\neq}$ and a more negative activation entropy $\Delta S^{\neq}$ due to the second binding of Sc^{3+} with more restricted geometry in the ET transition state as compared to pathway A to afford $TolSQ^{\bullet-}$–Sc^{3+}. Thus, we examined the temperature dependence of k_{et} at different Sc^{3+} concentrations (1.0×10^{-2} and 5.0×10^{-2} M). At a low concentration of Sc^{3+} (1.0×10^{-2} M) pathway A is dominant, whereas the contribution of the pathway B becomes predominant at a high concentration of Sc^{3+} (5.0×10^{-2} M). The resulting Eyring plots are shown in Figure 3. Nearly all TolSQ molecules form the TolSQ–Sc^{3+} complex in the presence of 5.0×10^{-2} M and 1.0×10^{-2} M of

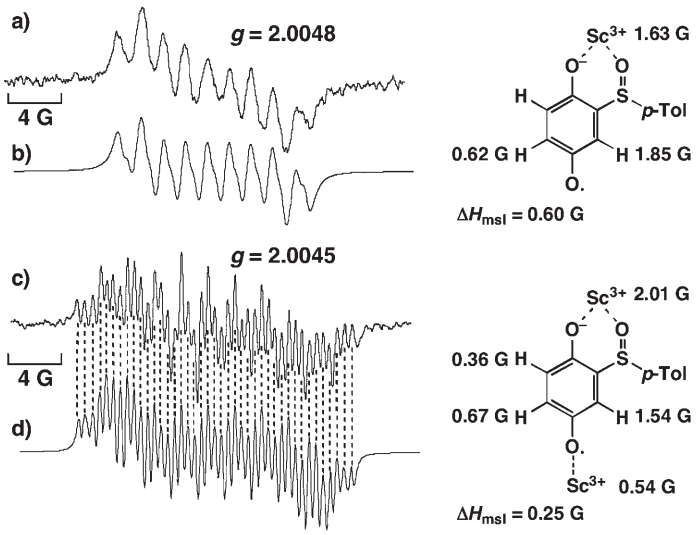

Figure 2. a) EPR spectrum of $TolSQ^{\bullet-}$–Sc^{3+} produced by ET from $(AcrH)_2$ (1.6×10^{-2} M) to TolSQ (4.2×10^{-2} M) in the presence of Sc^{3+} (4.2×10^{-3} M) and H_2O (4.6 M) in deaerated MeCN at 298 K and b) simulated spectrum. c) EPR spectrum of $TolSQ^{\bullet-}$–$(Sc^{3+})_2$ produced by ET from $(AcrH)_2$ (1.6×10^{-2} M) to TolSQ (4.3×10^{-2} M) in the presence of Sc^{3+} (2.1×10^{-1} M) and H_2O (2.4 M) in deaerated MeCN at 298 K and d) simulated spectrum. The hfc constants determined by computer simulation with ΔH_{msl} (maximum slope line width) are shown together with the structures of $TolSQ^{\bullet-}$–Sc^{3+} and $TolSQ^{\bullet-}$–$(Sc^{3+})_2$.

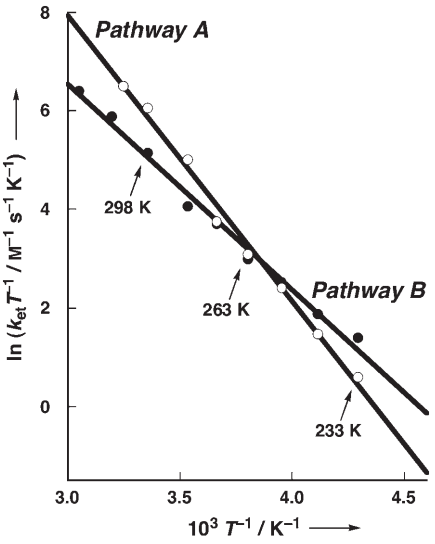

Figure 3. Plots of $\ln(k_{et}T^{-1})$ versus T^{-1} for ET from $(AcrH)_2$ (1.0×10^{-5} M) to TolSQ in the presence of $Sc(OTf)_3$ (1.0×10^{-2} M: open circles, 5.0×10^{-2} M: filled circles) in deaerated MeCN.

Sc^{3+} at 233–328 K judging from the large K_1 values at 298 and 233 K (vide supra). The activation enthalpies $\Delta H^{\neq}$ and entropies $\Delta S^{\neq}$ were determined from the slopes and the intercepts of the Eyring plots for ET as $\Delta H^{\neq}=(11.6\pm0.4)$ kcal mol^{-1} and $\Delta S^{\neq}=(3.2\pm1.5)$ cal mol^{-1} K^{-1} at low Sc^{3+} concentration (1.0×10^{-2} M), and $\Delta H^{\neq}=(8.3\pm0.3)$ kcal mol^{-1} and $\Delta S^{\neq}=(-9.4\pm1.1)$ cal mol^{-1} K^{-1} at high Sc^{3+} concentration (5.0×10^{-2} M). The larger $\Delta H^{\neq}$ value and positive $\Delta S^{\neq}$ value at low Sc^{3+} concentration (1.0×10^{-2} M) corresponds to pathway A. At a high concentration of Sc^{3+} (5.0×10^{-2} M), the contribution of pathway B becomes predominant with a smaller $\Delta H^{\neq}$ value and a more negative $\Delta S^{\neq}$ value because of the second binding of Sc^{3+} to $TolSQ^{\bullet-}$–Sc^{3+} to give $TolSQ^{\bullet-}$–$(Sc^{3+})_2$ (pathway B), which results in stronger binding and a higher degree of organization as compared with pathway A to afford the 1:1 $TolSQ^{\bullet-}$–Sc^{3+} complex.

The two plots cross at 263 K (Figure 3). In consequence, the k_{et} value increases with increasing Sc^{3+} concentration below 263 K, and decreases with increasing Sc^{3+} concentration above 263 K. At the crossing point, the k_{et} values remain constant with increasing Sc^{3+} concentration (Figure 1c).

If pathway A is independent of pathway B, k_{et} is given as the sum of the rate constants of pathways A (k_A) and B [k_B-$[Sc^{3+}]$, Eq. (2)].

$$k_{et} = k_A + k_B[Sc^{3+}] \quad (2)$$

In such a case, the k_{et} value would always increase with increasing concentration of Sc^{3+} irrespective of temperature. Thus, the observed decelerating effect of Sc^{3+} on the rate of ET from $(AcrH)_2$ to the TolSQ–Sc^{3+} complex at 298 K (Figure 1b) indicates that pathway A is not independent of pathway B. Pathway A thereby changes to the pathway B with increasing concentration of Sc^{3+} when k_{et} is given by Equation (3), where K_2 is the formation constant of the 1:2 complex $TolSQ^{\bullet-}$–$(Sc^{3+})_2$.

$$k_{et} = (k_A + k_B K_2[Sc^{3+}]^2)/(1 + K_2[Sc^{3+}]) \quad (3)$$

This is quite different from chemical reactions other than electron transfer. Because electron transfer occurs according to the Franck–Condon principle,[7,30] the ET transition state reflects the binding modes of the products, that is, $TolSQ^{\bullet-}$–Sc^{3+} (pathway A) and $TolSQ^{\bullet-}$–$(Sc^{3+})_2$ (pathway B).[31]

When $K_2[Sc^{3+}] \gg 1$, that is, pathway B is predominant over pathway A, Equation (3) reduces to Equation (4).

$$k_{et} = k_A K_2^{-1}[Sc^{3+}]^{-1} + k_B[Sc^{3+}] \quad (4)$$

The contribution of the second term $k_B[Sc^{3+}]$ as compared to the first term $k_A K_2^{-1}[Sc^{3+}]^{-1}$ will decrease with increasing temperature, because of the smaller $\Delta H^{\neq}$ value and the more negative $\Delta S^{\neq}$ value for pathway B (vide supra). In such a case Equation (4) reduces to Equation (5), which indicates that k_{et} is inversely proportional to concentration of Sc^{3+}, as observed in Figure 1b.

$$k_{et} = k_A K_2^{-1}[Sc^{3+}]^{-1} \quad (5)$$

Accelerating effect of Sc^{3+} on ET reduction of TolSQ and decelerating effect of Y^{3+} on ET reduction of PQ: Accelerating and decelerating effects of metal ions on the ET reduction of TolSQ may vary depending on the one-electron oxidation potentials of electron donors. Thus, we examined accelerating and decelerating effects of Sc^{3+} on the ET reduc-

tion of TolSQ by different electron donors with different one-electron oxidation potentials (vide infra).

When cobalt(II) tetraphenylporphyrin (CoTPP, $E_{ox}=$ 0.35 V versus SCE)[32] is employed as electron donor instead of $(AcrH)_2$ ($E_{ox}=0.62$ V versus SCE),[24] efficient ET from CoTPP to TolSQ ($E_{red}=-0.26$ V versus SCE)[25] also occurs in the presence of Sc^{3+} [Eq. (6)], whereas no ET occurs in the absence of Sc^{3+} due to a positive free-energy change ($\Delta G_{et}=0.61$ eV).[33]

$$\mathrm{CoTPP} + \mathrm{TolSQ} \xrightarrow{Sc^{3+}} [\mathrm{Co(TPP)}]^{+} + \mathrm{TolSQ}^{\cdot -} - (Sc^{3+})_n \quad (n = 1, 2) \tag{6}$$

The k_{et} value exhibits saturation behavior with respect to the concentration of Sc^{3+} at low concentrations of Sc^{3+} ($[Sc^{3+}]<5.0\times10^{-3}$ M) because of formation of the 1:1 complex of TolSQ with Sc^{3+} (TolSQ–Sc^{3+}), as seen in the case of ET from $(AcrH)_2$ (Figure 1). In contrast to the decelerating effect of Sc^{3+} on ET from $(AcrH)_2$ to TolSQ at 298 K (Figure 1b), the k_{et} value increases with increasing $[Sc^{3+}]$ at high concentrations of Sc^{3+} even at 298 K (Figure 4a). This indicates no changeover from an accelerating effect of Sc^{3+} to a decelerating effect below 298 K. Such a promoting effect of Sc^{3+} on ET has also been previously observed in ET from tris(2-phenylpyridine)iridium(III) [$Ir(ppy)_3$] to TolSQ,[25] which is shown in Figure 4b for comparison. The accelerating effect of Sc^{3+} on the ET reduction of TolSQ by CoTPP and $Ir(ppy)_3$ indicates a predominant contribution of the $k_B[Sc^{3+}]$ term in Equation (4) at 298 K.

We also examined the effect of Y^{3+} on the rate of ET from CoTPP ($E_{ox}=0.35$ V versus SCE)[32] to 9,10-phenanthrenequinone (PQ, $E_{red}=-0.65$ V versus SCE),[12b] because PQ also forms a 1:1 complex with Y^{3+} (PQ–Y^{3+}), like the case of TolSQ–Sc^{3+}.[34] No ET from CoTPP to PQ occurs in the absence of Y^{3+}, because the free energy change of ET is highly positive ($\Delta G_{et}=1.00$ eV). When PQ forms a 1:1 complex with Y^{3+} (PQ–Y^{3+}) and thus enhances the electron-acceptor ability of PQ, ET becomes possible [Eq. (7)].[12b,35]

$$\mathrm{CoTPP} + \mathrm{PQ} \xrightarrow{Y^{3+}} [\mathrm{Co(TPP)}]^{+} + \mathrm{PQ}^{\cdot -} - (Y^{3+})_n \quad (n = 1, 2) \tag{7}$$

Formation of the PQ–Y^{3+} complex was confirmed by UV/Vis spectral changes of PQ in the presence of various concentrations of Y^{3+} (see Figure S2 in the Supporting Information). In such a case, the second-order rate constant of ET k_{et} increases and exhibits saturation behavior with respect to $[Y^{3+}]$ at low concentrations of Y^{3+} ($[Y^{3+}]<3.0\times10^{-3}$ M) at 298 and 233 K (Figure 5a and b, respectively). At high concentrations of Y^{3+} ($[Y^{3+}]>5.0\times10^{-3}$ M) the k_{et} value decreases with increasing $[Y^{3+}]$ at both 298 and 233 K (Figure 5a and b, respectively).[36] Formation of the 1:1 complex ($PQ^{\cdot -}$–Y^{3+}) and the 1:2 complex ($PQ^{\cdot -}$–$(Y^{3+})_2$) in dependence on Y^{3+} concentration was also confirmed by EPR.[12b]

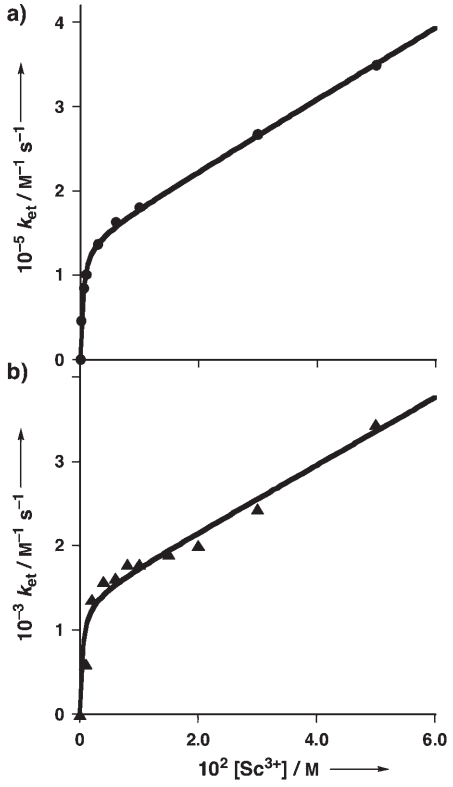

Figure 4. a) Dependence of k_{et} on $[Sc^{3+}]$ for ET from CoTPP (5.0×10^{-6} M) to TolSQ in the presence of Sc^{3+} in deaerated MeCN at 298 K. b) Dependence of k_{et} on $[Sc^{3+}]$ for ET from $Ir(ppy)_3$ (2.5×10^{-5} M) to TolSQ in the presence of Sc^{3+} in deaerated MeCN at 298 K.[25]

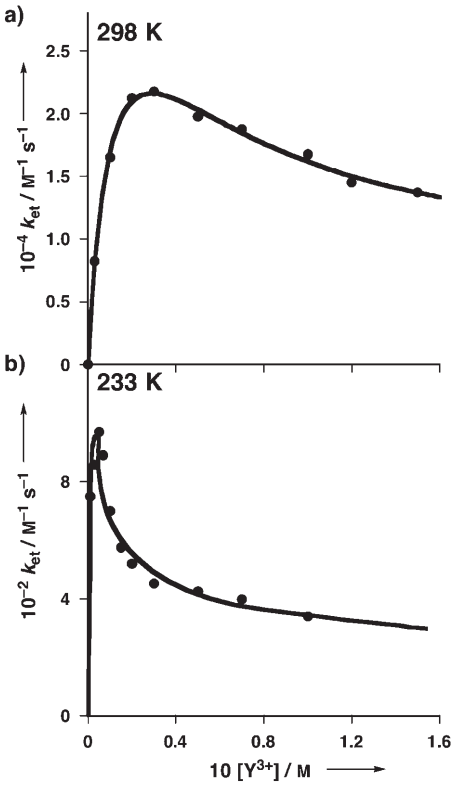

Figure 5. Dependence of k_{et} on $[Y^{3+}]$ for ET from CoTPP (1.0×10^{-6} M) to PQ in the presence of Y^{3+} in deaerated MeCN at a) 298 K and b) 233 K.

Thus, ET from CoTPP to PQ in the presence of Y^{3+} affords $PQ^{\bullet-}$–Y^{3+} (pathway A) and $PQ^{\bullet-}$–$(Y^{3+})_2$ (pathway B) at low and high concentrations of Y^{3+}, respectively (Scheme 3). Since Y^{3+} also has no effect on the oxidation potential of CoTPP, the decelerating effect of Y^{3+} on ET from CoTPP to PQ–Y^{3+} in Figure 5 results from the much smaller ET rate on pathway B than that on pathway A at 298 and 233 K.

The temperature dependences of k_{et}^0 ($=k_{et}(1+K[M^{n+}])/K[M^{n+}]$) for ET from CoTPP and $Ir(ppy)_3$ to TolSQ–Sc^{3+} and from CoTPP to PQ–Y^{3+} were also examined at high and low concentrations of metal ions ($M^{n+}=Sc^{3+}$, Y^{3+}). The k_{et}^0 correspond to second-order rate constants for ET from electron donors to TolSQ–Sc^{3+} and PQ–Y^{3+}, and the k_{et}^0 value is virtually the same as the k_{et} value under conditions such that $1 \ll K[M^{n+}]$.[37] The resulting Eyring plots at low and high concentrations of metal ions are shown in Figure 6 (open and filled symbols, respectively). In each case no crossing point is found in the temperature range between 233 and 333 K.

The activation parameters $\Delta H^{\neq}$ and $\Delta S^{\neq}$ of a series of ET reactions are listed in Table 1 together with the ΔG_{et} values.[38] Smaller $\Delta H^{\neq}$ and more negative $\Delta S^{\neq}$ values are obtained in the presence of higher concentrations of metal ions than in the presence of lower concentrations of metal ions in each case (Table 1). This results from stronger binding of metal ions and more restricted geometries in the ET transition states to afford the 1:2 complexes $TolSQ^{\bullet-}$–$(Sc^{3+})_2$ and $PQ^{\bullet-}$–$(Y^{3+})_2$ between radical anions and metal ions as compared with those to afford the 1:1 complexes $TolSQ^{\bullet-}$–Sc^{3+} and $PQ^{\bullet-}$–Y^{3+}.

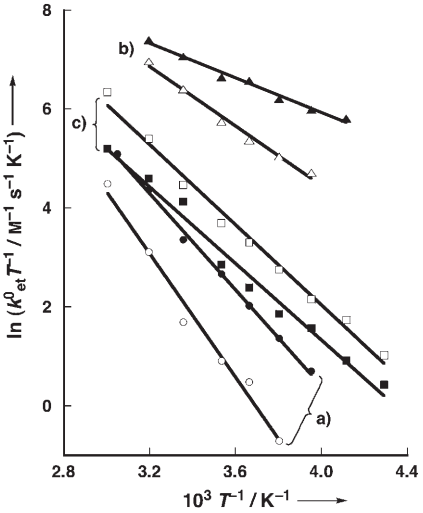

Figure 6. Plots of $\ln(k_{et}^0 T^{-1})$ versus T^{-1} for a) ET from $Ir(ppy)_3$ (2.5×10^{-5} M) to TolSQ in the presence of Sc^{3+} [1.0×10^{-2} M (open circles) and 1.0×10^{-1} M (filled circles)], b) ET from CoTPP (5.0×10^{-6} M) to TolSQ in the presence of Sc^{3+} [1.0×10^{-2} M (open triangles) and 5.0×10^{-2} M (filled triangles)], and c) ET from CoTPP (1.0×10^{-6} M) to PQ in the presence of Y^{3+} [2.0×10^{-2} M (open squares) and 1.0×10^{-1} M (filled squares)] in deaerated MeCN.

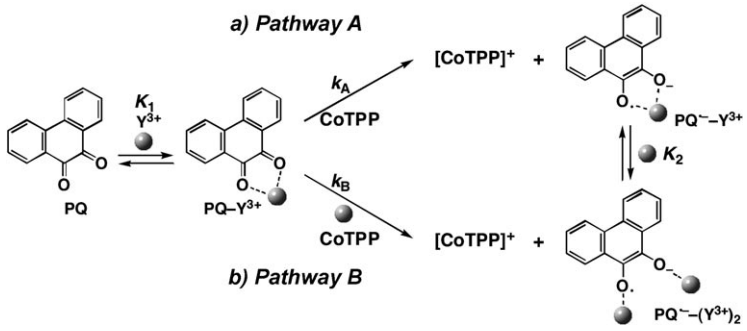

Scheme 3. ET from CoTPP to PQ–Y^{3+} to produce a) $PQ^{\bullet-}$–Y^{3+} and b) $PQ^{\bullet-}$–$(Y^{3+})_2$.

The $\Delta H^{\neq}$ values of the ET reduction of TolSQ at low and high concentrations of Sc^{3+} are plotted against the ET driving force $-\Delta G_{et}$ in Figure 7a. In both cases, the $\Delta H^{\neq}$ value decreases linearly with increasing $-\Delta G_{et}$, whereby the $\Delta H^{\neq}$ value in the presence of a high concentration of Sc^{3+} (filled circles) is smaller

Table 1. One-electron oxidation potentials E_{ox} of electron donors, one-electron reduction potentials E_{red} of electron acceptors in the presence of low and high concentrations of M^{n+}, free energy change ΔG_{et}, activation enthalpies $\Delta H^{\neq}$, and activation entropies $\Delta S^{\neq}$ of ET in the presence of low and high concentrations of M^{n+} in deaerated MeCN at 298 K.

No.	Electron donor	Electron acceptor	M^{n+}	E_{ox} [V vs. SCE]	E_{red} [V vs. SCE]		ΔG_{et} [eV]		$\Delta H^{\neq}$ [kcal mol^{-1}]		$\Delta S^{\neq}$ [cal mol^{-1} K^{-1}]	
					low conc[a]	high conc[b]	low conc[a]	high conc[b]	low conc[a]	high conc[b]	low conc[a]	high conc[b]
1	$Ir(ppy)_3$	TolSQ	Sc^{3+}	0.71	0.61[c,d]	0.65[d,e]	0.10[c]	0.06[e]	12.4 ± 0.8[c]	9.6 ± 0.3[e]	-1.4 ± 2.8[c]	-7.8 ± 0.8[e]
2	$(AcrH)_2$	TolSQ	Sc^{3+}	0.62	0.61[c,d]	0.63[d,f]	0.01[c]	−0.01[f]	11.6 ± 0.4[c]	8.3 ± 0.3[f]	3.2 ± 1.5[c]	-9.4 ± 1.1[f]
3	CoTPP	TolSQ	Sc^{3+}	0.35	0.61[c,d]	0.63[d,f]	−0.26[c]	−0.28[f]	6.0 ± 0.4[c]	3.5 ± 0.2[f]	-14.6 ± 1.2[c]	-21.6 ± 1.2[f]
4	CoTPP	PQ	Y^{3+}	0.35	0.40[g,h]	–[i]	−0.05[h]	–[i]	8.0 ± 0.3[h]	7.7 ± 0.4[j]	-11.0 ± 1.1[h]	-13.8 ± 1.4[j]

[a] Low concentrations of M^{n+}. [b] High concentrations of M^{n+}. [c] Value in the presence of 1.0×10^{-2} M of Sc^{3+}. [d] Determined from the equation $E_{red}=-0.26+0.059\log\{K_a(1+K_2[Sc^{3+}])/K_1\}$, where K_a is the formation constant of $TolSQ^{\bullet-}$–Sc^{3+}, and K_1 and K_2 are formation constants of TolSQ–Sc^{3+} and $TolSQ^{\bullet-}$–$(Sc^{3+})_2$, respectively; the K_a and K_2 values were taken as 1.3×10^{18} and 38 M^{-1}, respectively, from ref. [25]. [e] Value in the presence of 1.0×10^{-1} M of Sc^{3+}. [f] Value in the presence of 5.0×10^{-2} M of Sc^{3+}. [g] Taken from ref. [12b]. [h] Value in the presence of 2.0×10^{-2} M of Y^{3+}. [i] Not determined. [j] Value in the presence of 1.0×10^{-1} M of Y^{3+}.

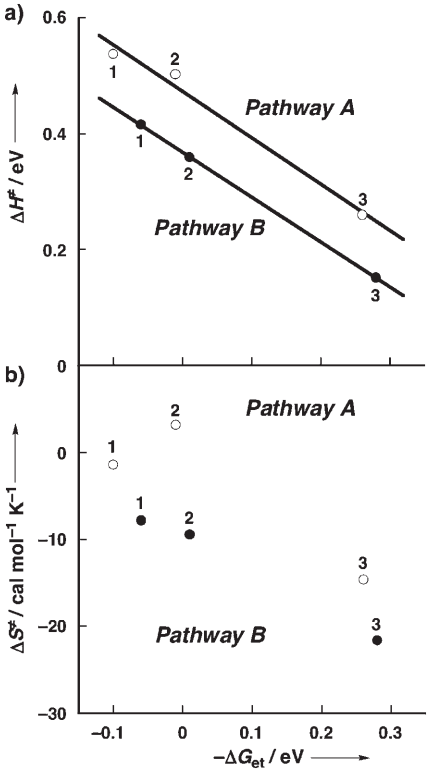

Figure 7. Plots of a) $\Delta H^{\neq}$ and b) $\Delta S^{\neq}$ versus $-\Delta G_{et}$ for ET from electron donors ($Ir(ppy)_3$, $(AcrH)_2$, and CoTPP) to TolSQ in the presence of low (1.0×10^{-2} M, open circles) and high (5.0×10^{-2} M or 1.0×10^{-1} M, filled circles) concentrations of Sc^{3+}. Numbers correspond to those given in Table 1.

than that in the presence of a lower concentration of Sc^{3+} (open circles) irrespective of the $-\Delta G_{et}$ value. In contrast, the relation between $\Delta S^{\neq}$ and $-\Delta G_{et}$ (Figure 7b) is not so simple as the linear correlation between $\Delta H^{\neq}$ and $-\Delta G_{et}$ (Figure 7a), because the transition-state geometry may be different depending on the type of electron donors. The difference in the $\Delta S^{\neq}$ values between pathways A and B is the largest for the case of $(AcrH)_2$ (no. 2 in Figure 7b). This is the reason why a crossing point occurs at 263 K in Eyring plots (Figure 3). In the other cases, the extrapolated crossing temperature is too high or too low to be observed in the limited range of temperature (233–333 K) in Figure 6.

In the case of ET from CoTPP to PQ in the presence of Y^{3+}, the $\Delta H^{\neq}$ value of pathway B (7.7 ± 0.4 kcal mol^{-1}) is only slightly smaller than that of pathway A (8.0 ± 0.3 kcal mol^{-1}; Table 1). Such a slight difference in the $\Delta H^{\neq}$ value between pathways A and B may result from the binding modes of $PQ^{\bullet-}$–Y^{3+} and $PQ^{\bullet-}$–$(Y^{3+})_2$ (vide infra). The second binding of Y^{3+} to $PQ^{\bullet-}$–Y^{3+} dissociates a chelate ring of $PQ^{\bullet-}$–Y^{3+} to allow $PQ^{\bullet-}$–$(Y^{3+})_2$ to form (Scheme 3), which results in weaker second binding than that of Sc^{3+} to $TolSQ^{\bullet-}$–Sc^{3+} to afford $TolSQ^{\bullet-}$–$(Sc^{3+})_2$. Such a weak second binding of Y^{3+} reflects a subtle difference in the binding enthalpy between $PQ^{\bullet-}$–Y^{3+} and $PQ^{\bullet-}$–$(Y^{3+})_2$ in relation to the difference in $\Delta H^{\neq}$ values between pathways A and B (Scheme 3).

Conclusions

We have demonstrated the accelerating and decelerating effects of metal ions on the ET reduction of quinones as a function of temperature in relation to binding modes of metal ions to semiquinone radical anions. The quinone derivatives TolSQ and PQ employed as electron acceptors form 1:1 complexes with Sc^{3+} and Y^{3+} (TolSQ–Sc^{3+} and PQ–Y^{3+}, respectively). Formation of TolSQ–Sc^{3+} and PQ–Y^{3+} complexes enables efficient ET reduction of TolSQ and PQ by electron donors such as CoTPP. The resulting ET products $TolSQ^{\bullet-}$–Sc^{3+} and $PQ^{\bullet-}$–Y^{3+} are converted to the 1:2 complexes $TolSQ^{\bullet-}$–$(Sc^{3+})_2$ and $PQ^{\bullet-}$–$(Y^{3+})_2$ at higher concentrations of metal ions. The conversion of $TolSQ^{\bullet-}$–Sc^{3+} to $TolSQ^{\bullet-}$–$(Sc^{3+})_2$ with increasing Sc^{3+} concentration has been successfully observed by EPR. The ET pathway B to afford the 1:2 complexes has smaller activation enthalpies $\Delta H^{\neq}$ and more negative activation entropies $\Delta S^{\neq}$ because of stronger binding of metal ions and more restricted geometries of the ET transition states as compared to ET pathway A to afford the 1:1 complexes. Such differences in the $\Delta H^{\neq}$ and $\Delta S^{\neq}$ values generally result in crossing of the Eyring plots of ET pathways A and B. In the case of ET from $(AcrH)_2$ to the TolSQ–Sc^{3+} complex, crossing of the two Eyring plots is experimentally observed at 263 K. At the lower temperature, the ET rate increases with increasing concentration of Sc^{3+}, whereas at the higher temperature this is reversed, that is, the ET rate decreases with increasing concentration of Sc^{3+}. At 263 K, the ET rate remains constant with increasing concentration of Sc^{3+}. Thus, it has been shown for the first time that metal ions exhibit both accelerating and decelerating effects on ET, depending on the difference in temperature in relation to the binding modes of metal ions to the ET products (radical anions).

Experimental Section

Materials: 1-(*p*-Tolylsulfinyl)-2,5-benzoquinone (TolSQ),[39] cobalt(II) tetraphenylporphyrin (CoTPP),[40] and tris(2-phenylpyridine)iridium [Ir(ppy)$_3$][41] were prepared according to the literature. 10,10′-Dimethyl-9,9′-biacridine ($(AcrH)_2$) was prepared by one-electron reduction of 10-methylacridinium perchlorate with hexamethylditin.[42] 9,10-Phenanthrenequinone (PQ) was obtained commercially and purified by the standard methods.[43] Scandium triflate [$Sc(OTf)_3$] (99%) was purchased from Pacific Metals Co., Ltd. (Taiheiyo Kinzoku). Yttrium triflate [$Y(OTf)_3$] was obtained from Acros. Acetonitrile (MeCN) used as solvent was purified and dried by the standard procedure.[43]

Spectral measurements: Formation of the Y^{3+} complex with PQ (PQ–Y^{3+}) was monitored by means of the change in the UV/Vis spectra of PQ in the presence of various concentrations of Y^{3+} at 233–333 K on a Hewlett Packard 8453 diode array spectrophotometer.

Kinetic measurements: Kinetic measurements were performed by using a Unisoku RSP-601 stopped-flow spectrophotometer with an MOS-type high-sensitivity photodiode array. Rates of ET from CoTPP (5.0×10^{-6} M) to TolSQ (5.0×10^{-5} M) in the presence of Sc^{3+} (0–5.0×10^{-2} M) and ET from CoTPP (1.0×10^{-6} M) to PQ (4.0×10^{-5} M) in the presence of Y^{3+} (0–1.5×10^{-1} M) were monitored by the rise of the absorption band at 434 nm due to $CoTPP^{+}$ in deaerated MeCN at 233–333 K. Rates of ET from $(AcrH)_2$ (1.0×10^{-5} M) to TolSQ (2.0×10^{-4} M) in the presence of Sc^{3+} (0–

1.0×10^{-1} M) were monitored by the increase in the absorption band due to 10-methylacridinium ion ($AcrH^+$: $\lambda_{max}=358$ nm, $\varepsilon_{max}=1.80\times10^4$ $M^{-1}cm^{-1}$)[24] in deaerated MeCN at 233–328 K in the dark. Rates of electron transfer from $Ir(ppy)_3$ (2.5×10^{-5} M) to TolSQ (5.0×10^{-4} M) in the presence of Sc^{3+} (0–5.0×10^{-2} M) were monitored by the rise and decay of the absorption bands at 580 and 380 nm due to $[Ir(ppy)_3]^+$ and $Ir(ppy)_3$, respectively, in deaerated MeCN at 253–328 K.

EPR measurements: EPR spectra of Sc^{3+} complexes of $TolSQ^{\bullet-}$ were recorded on a JEOL JES-RE1XE spectrometer in a sample cell in the EPR cavity at 298 K. Typically, TolSQ (8.4×10^{-2} M) was dissolved in deaerated MeCN and purged with argon for 10 min. $Sc(OTf)_3$ (8.4×10^{-3} M in 1.0 mL) was dissolved in deaerated MeCN. The TolSQ (200 mL) and Sc^{3+} (200 mL) solutions in MeCN were introduced into an EPR cell (1.8 mm i.d.) containing $(AcrH)_2$ (1.6×10^{-2} M) and mixed by bubbling with Ar gas through a syringe with a long needle. The magnitude of modulation was chosen to optimize the resolution and signal-to-noise ratio of observed spectra under conditions of nonsaturating microwave power. The *g* values and hyperfine coupling constants were calibrated with a Mn^{2+} marker. Computer simulation of the ESR spectra was carried out by using Calleo ESR version 1.2 (Calleo Scientific Publisher) on a personal computer.

Acknowledgements

This work was partially supported by Grants-in-Aid (Nos. 19205019) from the Ministry of Education, Culture, Sports, Science and Technology, Japan.

[1] a) W. Kaim, B. Schwederski, *Bioinorganic Chemistry: Inorganic Elements in the Chemistry of Life*, Wiley, New York, **1994**; b) S. Ferguson-Miller, G. T. Babcock, *Chem. Rev.* **1996**, *96*, 2889–2907; c) R. H. Holm, P. Kennepohl, E. I. Solomon, *Chem. Rev.* **1996**, *96*, 2239–2314.

[2] a) L. M. Utschig, M. C. Thurnauer, *Acc. Chem. Res.* **2004**, *37*, 439–447; b) S. Hermes, O. Bremm, F. Garczarek, V. Derrien, P. Liebisch, P. Loja, P. Sebban, K. Gerwert, M. Haumann, *Biochemistry* **2006**, *45*, 353–359.

[3] a) V. M. Rotello in *Electron Transfer in Chemistry, Vol. 4* (Ed.: V. Balzani), Wiley-VCH, Weinheim, **2001**, pp. 68–87; b) M. Gray, A. O. Cuello, G. Cooke, V. M. Rotello, *J. Am. Chem. Soc.* **2003**, *125*, 7882–7888; c) D. J. Duffy, K. Das, S. L. Hsu, J. Penelle, V. M. Rotello, H. D. Stidham, *J. Am. Chem. Soc.* **2002**, *124*, 8290–8296.

[4] a) J. Breton, C. Boullais, J.-R. Burie, E. Nabedryk, C. Mioskowski, *Biochemistry* **1994**, *33*, 14378–14386; b) B. A. Diner, D. A. Force, D. W. Randall, R. D. Britt, *Biochemistry* **1998**, *37*, 17931–17943; c) H. Ishikita, E.-W. Knapp, *J. Am. Chem. Soc.* **2004**, *126*, 8059–8064.

[5] a) K. Okamoto, K. Ohkubo, K. M. Kadish, S. Fukuzumi, *J. Phys. Chem. A* **2004**, *108*, 10405–10413; b) S. Fukuzumi, Y. Yoshida, K. Okamoto, H. Imahori, Y. Araki, O. Ito, *J. Am. Chem. Soc.* **2002**, *124*, 6794–6795; c) S. Fukuzumi, K. Okamoto, Y. Yoshida, H. Imahori, Y. Araki, O. Ito, *J. Am. Chem. Soc.* **2003**, *125*, 1007–1013; d) S. Fukuzumi, H. Kitaguchi, T. Suenobu, S. Ogo, *Chem. Commun.* **2002**, 1984–1985; e) K. Okamoto, S. Fukuzumi, *J. Phys. Chem. B* **2005**, *109*, 7713–7723; f) J. Yuasa, S. Yamada, S. Fukuzumi, *Angew. Chem.* **2007**, *119*, 3623–3625; *Angew. Chem. Int. Ed.* **2007**, *46*, 3553–3555.

[6] a) H. B. Gray, J. R. Winkler, *Annu. Rev. Biochem.* **1996**, *65*, 537–561; b) R. Langen, I.-J. Chang, J. P. Germanas, J. H. Richards, J. R. Winkler, H. B. Gray, *Science* **1995**, *268*, 1733–1735; c) J. R. Winkler, H. B. Gray, *Chem. Rev.* **1992**, *92*, 369–379.

[7] a) S. Fukuzumi in *Electron Transfer in Chemistry, Vol. 4* (Ed.: V. Balzani), Wiley-VCH, Weinheim, **2001**, pp. 3–67; b) S. Fukuzumi, *Org. Biomol. Chem.* **2003**, *1*, 609–620; c) S. Fukuzumi, *Bull. Chem. Soc. Jpn.* **1997**, *70*, 1–28.

[8] a) S. Itoh, H. Kawakami, S. Fukuzumi, *J. Am. Chem. Soc.* **1998**, *120*, 7271–7277; b) S. Itoh, H. Kawakami, S. Fukuzumi, *J. Am. Chem. Soc.* **1997**, *119*, 439–440; c) S. Itoh, H. Kawakami, S. Fukuzumi, *Biochemistry* **1998**, *37*, 6562–6571.

[9] a) S. Fukuzumi, N. Nishizawa, T. Tanaka, *J. Chem. Soc. Perkin Trans. 2* **1985**, 371–378; b) S. Fukuzumi, T. Okamoto, J. Otera, *J. Am. Chem. Soc.* **1994**, *116*, 5503–5504; c) S. Fukuzumi, S. Itoh in *Advances in Photochemistry, Vol. 25* (Eds.: D. C. Neckers, D. H. Volman, G. von Bünau), Wiley, New York, **1998**, pp. 107–172.

[10] S. Fukuzumi, J. Yuasa, T. Suenobu, *J. Am. Chem. Soc.* **2002**, *124*, 12566–12573.

[11] S. Fukuzumi, J. Yuasa, T. Miyagawa, T. Suenobu, *J. Phys. Chem. A* **2005**, *109*, 3174–3181.

[12] a) J. Yuasa, T. Suenobu, S. Fukuzumi, *J. Am. Chem. Soc.* **2003**, *125*, 12090–12091; b) J. Yuasa, T. Suenobu, S. Fukuzumi, *ChemPhysChem* **2006**, *7*, 942–954; c) J. Yuasa, T. Suenobu, S. Fukuzumi, *J. Phys. Chem. A* **2005**, *109*, 9356–9362; d) K. Okamoto, S. Fukuzumi, *J. Am. Chem. Soc.* **2003**, *125*, 12416–12417.

[13] a) S. Fukuzumi, K. Ohkubo, T. Okamoto, *J. Am. Chem. Soc.* **2002**, *124*, 14147–14155; b) S. Fukuzumi, Y. Fujii, T. Suenobu, *J. Am. Chem. Soc.* **2001**, *123*, 10191–10199; c) J. Yuasa, T. Suenobu, K. Ohkubo, S. Fukuzumi, *Chem. Commun.* **2003**, 1070–1071; d) K. Okamoto, H. Imahori, S. Fukuzumi, *J. Am. Chem. Soc.* **2003**, *125*, 7014–7021.

[14] S. Fukuzumi, J. Yuasa, N. Satoh, T. Suenobu, *J. Am. Chem. Soc.* **2004**, *126*, 7585–7594.

[15] H. Wu, D. Zhang, L. Su, K. Ohkubo, C. Zhang, S. Yin, L. Mao, Z. Shuai, S. Fukuzumi, D. Zhu, *J. Am. Chem. Soc.* **2007**, *129*, 6839–6846.

[16] a) A. A. Milischuk, D. V. Matyushov, M. D. Newton, *Chem. Phys.* **2006**, *324*, 172–194; b) P. K. Ghorai, D. V. Matyushov, *J. Phys. Chem. A* **2006**, *110*, 8857–8863; c) D. V. Matyushov, *Acc. Chem. Res.* **2007**, *40*, 294–301.

[17] M. B. Zimmt, D. H. Waldeck, *J. Phys. Chem. A* **2003**, *107*, 3580–3597.

[18] a) M. Wanner, T. Sixt, K.-W. Klinkhammer, W. Kaim, *Inorg. Chem.* **1999**, *38*, 2753–2755; b) B. Schwederski, V. Kasack, W. Kaim, E. Roth, J. Jordanov, *Angew. Chem.* **1990**, *102*, 74–76; *Angew. Chem. Int. Ed. Engl.* **1990**, *29*, 78–79; c) S. Ernst, P. Hänel, J. Jordanov, W. Kaim, V. Kasack, E. Roth, *J. Am. Chem. Soc.* **1989**, *111*, 1733–1738; d) S. Ghumaan, B. Sarkar, S. Patra, J. van Slageren, J. Fiedler, W. Kaim, G. K. Lahiri, *Inorg. Chem.* **2005**, *44*, 3210–3214.

[19] For X-ray crystallography of contact and separated ion pairs of alkali metal salts of radical anions, see: a) J.-M. Lü, S. V. Rosokha, S. V. Lindeman, I. S. Neretin, J. K. Kochi, *J. Am. Chem. Soc.* **2005**, *127*, 1797–1809; b) M. G. Davlieva, J.-M. Lü, S. V. Lindeman, J. K. Kochi, *J. Am. Chem. Soc.* **2004**, *126*, 4557–4565; c) S. V. Rosokha, J.-M. Lü, M. D. Newton, J. K. Kochi, *J. Am. Chem. Soc.* **2005**, *127*, 7411–7420; d) J.-M. Lü, S. V. Rosokha, I. S. Neretin, J. K. Kochi, *J. Am. Chem. Soc.* **2006**, *128*, 16708–16719.

[20] *The Chemistry of Quinonoid Compounds* (Ed.: S. Patai), Wiley, New York, **1974**.

[21] a) *Functions of Quinones in Energy Conserving Systems* (Ed.: B. I. Trumpower), Academic Press, New York, **1986**; b) R. E. Blankenship, *Molecular Mechanism of Photosynthesis*, Blackwell, Cambridge, **2001**.

[22] a) M. L. Paddock, S. H. Rongey, G. Feher, M. Y. Okamura, *Proc. Natl. Acad. Sci. USA* **1989**, *86*, 6602–6606; b) P. Ädelroth, M. L. Paddock, L. B. Sagle, G. Feher, M. Y. Okamura, *Proc. Natl. Acad. Sci. USA* **2000**, *97*, 13086–13091.

[23] Scandium and yttrium ions are known to have relatively strong Lewis acidity. Since rare earth metal ions such as Y^{3+} are known to have similar Lewis acidity, the other lanthanide ions may be generally applicable to the present reaction system: S. Fukuzumi, K. Ohkubo, *Chem. Eur. J.* **2000**, *6*, 4532–4535.

[24] S. Fukuzumi, Y. Tokuda, *J. Phys. Chem.* **1992**, *96*, 8409–8413.

[25] J. Yuasa, S. Yamada, S. Fukuzumi, *J. Am. Chem. Soc.* **2006**, *128*, 14938–14948.

[26] S. Fukuzumi, K. Ohkubo, Y. Tokuda, T. Suenobu, *J. Am. Chem. Soc.* **2000**, *122*, 4286–4294.
[27] S. Fukuzumi, S. Koumitsu, K. Hironaka, T. Tanaka, *J. Am. Chem. Soc.* **1987**, *109*, 305–316.
[28] Higher resolution hyperfine structures of the $TolSQ^{\bullet-}$–Sc^{3+} and $TolSQ^{\bullet-}$–$(Sc^{3+})_2$ complexes are observed in the presence of a small amount of water, because self-exchange ET with neutral TolSQ, which results in an increase in the line width, may be slowed down.[25]
[29] $TolSQ^{\bullet-}$ was produced by photoinduced ET from $(AcrH)_2$ to TolSQ. The hyperfine splittings due to three protons (a(3 H) = 2.00, 2.20, and 3.35 G) and g value (g = 2.0057) of $TolSQ^{\bullet-}$ are changed by complex formation with Sc^{3+}.[25]
[30] a) R. A. Marcus, *Annu. Rev. Phys. Chem.* **1964**, *15*, 155–196; b) R. A. Marcus, *Angew. Chem.* **1993**, *105*, 1161–1172; *Angew. Chem. Int. Ed. Engl.* **1993**, *32*, 1111–1121.
[31] One might think that the rate-determining step in the presence of a large concentration of Sc^{3+} is ET from $(AcrH)_2$ to TolSQ–Sc^{3+}, followed by the rapid binding of additional Sc^{3+} to $TolSQ^{\bullet-}$–Sc^{3+} to afford $TolSQ^{\bullet-}$–$(Sc^{3+})_2$. However, this is certainly not the case for metal-ion-promoted ET reactions, where an additional Sc^{3+} ion is also involved in the rate-determining step.
[32] S. Fukuzumi, S. Mochizuki, T. Tanaka, *Inorg. Chem.* **1989**, *28*, 2459–2465.
[33] Metal ions have no effect on the oxidation potentials of CoTPP and $[Ir(ppy)_3]$.
[34] Y^{3+} was chosen instead of Sc^{3+}, because no 1:2 complex is formed between $PQ^{\bullet-}$ and Sc^{3+} even at a high concentration of Sc^{3+} (8.1×10^{-1} M); see ref. [12b].
[35] In the presence of 2.0×10^{-2} M of Y^{3+}, the reduction potential of PQ is shifted to 0.40 V (versus SCE); see ref. [12b].
[36] In contrast to the case of Y^{3+}, the k_{et} value of ET from CoTPP to PQ in the presence of Sc^{3+} exhibits saturation dependence with respect to Sc^{3+} concentration due to formation of a 1:1 PQ–Sc^{3+} complex; see ref. [12b].
[37] In contrast to strong complex formation of TolSQ with Sc^{3+}, the observed k_{et} values at low concentrations of Y^{3+} are smaller than those of ET from CoTPP to the PQ–Y^{3+} complex because of the smaller K_1 value of the PQ–Y^{3+} complex (e.g. $K=2.0\times10^2\,M^{-1}$ at 233 K, see Figure S2). Thus, we employed k_{et}^0 $\{=k_{et}(1+K[M^{n+}])/K[M^{n+}]\}$ in the Eyring plots (Figure 6).
[38] The ET from $(AcrH)_2$ (E_{ox} = 0.62 V versus SCE) to TolSQ in the presence of 1.0×10^{-2} M of Sc^{3+} is still slightly uphill (ΔG_{et} = 0.01 eV, Table 1), but the ET equilibrium may lie to the products side under pseudo-first-order conditions when concentrations of TolSQ and Sc^{3+} are maintained at more than ten times that of $(AcrH)_2$.
[39] a) H. Grennberg, A. Gogoll, J.-E. Bäckvall, *J. Org. Chem.* **1991**, *56*, 5808–5811; b) M. C. Carreño, J. L. García-Ruano, A. Urbano, *Tetrahedron Lett.* **1989**, *30*, 4003–4006.
[40] A. Shirazi, H. M. Goff, *Inorg. Chem.* **1982**, *21*, 3420–3425.
[41] K. Dedeian, P. I. Djurovich, F. O. Garces, G. Carlson, R. J. Watts, *Inorg. Chem.* **1991**, *30*, 1685–1687.
[42] S. Fukuzumi, T. Kitano, K. Mochida, *J. Am. Chem. Soc.* **1990**, *112*, 3246–3247.
[43] W. L. F. Armarego, C. L. L. Chai, *Purification of Laboratory Chemicals*, 5th ed., Butterworth Heinemann, Amsterdam, **2003**.

Received: September 8, 2007
Published online: December 11, 2007

